The Vesicle–Micelle Transition in Mixed Lipid–Surfactant Systems: A Molecular Model

Deborah R. Fattal,[†] David Andelman,[‡,§] and Avinoam Ben-Shaul*,[†]

Department of Physical Chemistry and The Fritz Haber Research Center, The Hebrew University of Jerusalem, Jerusalem 91904, Israel, School of Physics and Astronomy, Raymond and Beverly Sackler Faculty of Exact Sciences, Tel-Aviv University, Ramat Aviv, Tel-Aviv 69978, Israel, and Section de Physique et Chimie, Institut Curie, 11 rue P. et M. Curie, 75231 Paris Cedex 05, France

Received October 13, 1994. In Final Form: January 26, 1995[⊗]

A molecular model is used to calculate the free energy of mixed vesicles and cylindrical micelles, composed of lipid molecules and short chain surfactants. The free energy of both aggregates (modeled as an infinite planar bilayer and an infinite cylindrical aggregate) is represented as a sum of internal free energy and mixing entropy contributions. The internal free energy is treated as a sum of chain (conformational), head group, and surface tension terms. Calculating the free energy of each aggregation geometry as a function of lipid/surfactant composition and using common tangent construction we obtain the compositions of the bilayer and the micelle at the phase transition. By varying certain molecular parameters (such as the "hard core" area of the surfactant head group or the length of the surfactant tail) we study the role of molecular packing characteristics in determining the compositions at phase coexistence. We find, as expected, that upon increasing the preference of the surfactant for the micellar geometry (larger *spontaneous curvature*) the bilayer is solubilized at lower surfactant/lipid concentration ratios. For some typical values of the parameters used, reasonable agreement with experimental results for mixtures of egg phosphatidylcholine and octylglucoside is obtained.

1. Introduction

The structure, thermodynamics, and dynamic properties of aggregates or films of amphiphilic molecules are of prime importance in a great variety of systems.[1] For instance, the phase behavior of microemulsions depends in a sensitive way on the molecular composition and hence on the elastic properties of the surfactant–cosurfactant films separating the oil and water domains.[1] Similarly, the shapes, elastic properties, and phase transitions in biological membranes depend critically on their lipid composition and the presence of *solutes* such as proteins and cholesterol.[2] Another well-studied example is the vesicle–micelle transition attendant upon the incorporation of certain surfactants (detergents) into phospholipid vesicles, a process of importance, for example, in membrane reconstitution.[3–12]

The vesicle–micelle transition which, in recent years, has been studied by various experimental techniques is also the subject matter of the theoretical model presented in this paper. More specifically, our objective is to demonstrate, on the basis of molecular considerations, the role of packing constraints and intermolecular interactions in determining the equilibrium geometry (curvature) of mixed self-assembling aggregates, and their possible influence on first-order phase transitions from one aggregation geometry to another.

Light scattering and other experiments have revealed, some time ago, that the addition of bile salts to phospholipid bilayers results, above a certain surfactant to lipid ratio, in the destablilization of the vesicular structures and the formation of relatively small micelles.[3–8] It has been suggested that the micelles are disklike objects with the surfactant preferably situated at their edges, but also within their disklike body.[5] Recent cryotransmission electron microscopy experiments,[9] on phosphatidylcholine–octyl glucoside (PC–OG) mixtures, demonstrate clearly that in these systems, above a certain (*saturation*) OG to PC ratio, the lipid bilayer is *solubilized* into wormlike (cylindrical) micelles. After the solubilization is completed, and the system is composed entirely of cylindrical micelles, further addition of OG results in "fragmentation" of the wormlike micelles. At even higher surfactant mole fractions, the micelles become spheroidal.[9] This trend is consistent with the observation that pure octyl glucoside molecules in water form, above the critical micelle concentration (*cmc*), small spheroidal micelles.[13,14] Qualitatively similar behavior has been observed in other

[†] The Hebrew University of Jerusalem.
[‡] Tel-Aviv University.
[§] Institut Curie.
[⊗] Abstract published in *Advance ACS Abstracts,* April 1, 1995.

(1) For reviews, see: (a) Corti, M.; Degiorgio, V. (Eds.) *Physics of Amphiphiles: Micelles, Vesicles and Microemulsions*; North-Holland: Amsterdam, 1985. (b) Langevin, D.; Meunier, J.; Boccara, N. (Eds.) *Physics of Amphiphilic Layers*; Springer: Berlin, 1987. (c) Gelbart, W. M.; Ben-Shaul A.; Roux, D. (Eds.) *Micelles Membranes, Microemulsions and Monolayers*; Springer: New York, 1994. (d) Safran, S. A. *Statistical Thermodynamics of Surfaces, Interfaces and Membranes*; Addison Wesley: Reading, MA, 1994. (e) Lipowsky, R.; Sackmann, E. (Eds.) *Structure and Dynamics of Membranes*; Elsevier: Amsterdam, 1994.

(2) For reviews, see: Bloom, M.; Evans, E.; Mouritsen, O. *Q. Rev. Biophys.* **1991**, *24*, 193. Mouritsen, O.; Bloom, M. *Ann. Rev. Biophys. Biomol. Struct.* **1993**, *22*, 145.

(3) For a recent review on lipid/surfactant systems, see: Lichtenberg, D. In *Biomembranes: Physical Aspects*; Shinitzky, M., Ed.; VCH Balaban Publishers: Weinheim, 1993, Chapter 3 and references therein.

(4) Small, D. M. *The Physical Chemistry of Lipids*; Plenum: New York, 1986, and references therein.

(5) Shurtenberger, P.; Mazer, N. in ref 1a. Shurtenberger, P.; Mazer, N.; Känzig, W. *J. Phys. Chem.* **1985**, *89*, 1042.

(6) Almog, S.; Kushnir, T.; Nir, S.; Lichtenberg, D. *Biochemistry* **1986**, *25*, 2597.

(7) Fromherz, P.; Röcker, C.; Rüppel, D. *Faraday Discuss. Chem. Soc.* **1986**, *81*, 39.

(8) Walter, A.; Vinson, P. K.; Kaplan, A.; Talmon, Y. *Biophys. J.* **1991**, *60*, 1315.

(9) Vinson, P. K.; Talmon, Y.; Walter, W. *Biophys. J.* **1989**, *56*, 669.

(10) Ollivon, M.; Eidelman, O.; Blumenthal, R.; Walter, A. *Biochemistry* **1988**, *27*, 1695. See also; Eidelman, O.; Blumenthal, R.; Walter, A. *Biochemistry* **1988**, *27*, 2839.

(11) Paternostre, M. T.; Roux, M.; Rigaud, J. L. *Biochemistry* **1988**, *27*, 2668.

(12) Almog, S.; Litman, B. J.; Wimley, W.; Cohen, J.; Wachtel, E.; Barenholz, E. J.; Ben-Shaul, A.; Lichtenberg, D. *Biochemistry* **1990**, *29*, 4582.

(13) Rosevear, P.; VanAken, T.; Baxter, J.; Ferguson-Miller, S. *Biochemistry* **1980**, *19*, 4108. VanAken, T.; Foxall-VanAken, S.; Castleman, S.; Ferguson-Miller, S. *Methods Enzymol.* **1986**, *125*, 27.

0743-7463/95/2411-1154$09.00/0

systems, e.g. in mixtures of lecithins and the nonionic surfactant $C_{12}E_8$ (octaethylene glycol *n*-dodecyl monother).[15]

A theoretical model of the vesicle–micelle transition for lipid/surfactant mixtures has recently been proposed[16] based on concepts from continuum theory of curvature elasticity of thin films.[17] The key idea in this approach is that the spontaneous curvature of an amphiphilic aggregate varies (linearly) with its lipid–surfactant composition, ranging from that of a (nearly) planar bilayer for a pure lipid system to that of a cylindrical micelle in the limit of a pure surfactant system. By adding the mixing entropy contribution to the aggregate free energy it has been shown that a first-order phase transition from a vesicle to a cylindrical micelle can indeed take place. The compositions of the two coexisting phases (an infinite bilayer and an infinite cylindrical micelle) can be determined by a common tangent construction. A limitation of this model is the use of the quadratic elastic free energy, valid for small curvature deformations, to describe the internal (packing) free energy in both the planar bilayer and the highly curved cylindrical geometry.

In this paper we adopt a molecular approach for calculating the free energy of mixed, self-assembled, amphiphilic aggregates, valid for planar films (bilayers, monolayers) as well as for highly curved aggregates such as cylindrical or spherical micelles.[18,19] As in ref 16 the vesicle–micelle transition will be treated as a phase transition between two macroscopic phases: a planar bilayer (assuming that the vesicle radius is much larger than its bilayer thickness) and a long cylindrical aggregate (thus ignoring edge effects and polydispersity). The free energy differences involved typically in the vesicle–micelle transition are on the order of kT per molecule (section 3). On the other hand, the curvature free energy of a vesicle relative to a planar bilayer is $2\pi\kappa$, with $\kappa \sim (10-50)kT$ denoting the bending elastic modulus. For a vesicle of radius, say, $R = 500$ Å in which the average area per lipid chain is ~ 35 Å^2, this implies a bending free energy of less than 0.01 kT/molecule. Hence, representing the vesicle as a planar bilayer is a minor approximation.

The vesicle–micelle transition is necessarily of first order due to the very different symmetries of the two phases. The free energy of the molecules in the bilayer and in the cylindrical phase will be calculated as a sum of "internal" free energy contributions and an entropy of mixing term. The internal free energy will be treated as a sum of head group, interfacial, and hydrocarbon tail (conformational) free energies, all three depending on the lipid–surfactant composition, as detailed in section 2. Then, the vesicle and micelle concentrations at phase coexistence will be determined by common tangent construction. By varying some of the molecular parameters, such as the surfactant chain length and the size of the polar head groups, which tune the preferred packing geometry of the constituent molecules, we shall try to examine the role of the *spontaneous curvature* in the shape transformation from a vesicle to a micelle.

The model described in the next section does not take into account certain effects which may play a role in determining the exact compositions at coexistence. Namely, we do not include the translational entropy of the vesicles or the cylindrical micelles in the aqueous solution nor the effects of size polydispersity, composition, or shape fluctuations and interaggregate interactions. We also ignore the possible (small) variations in the free monomer concentrations in the solution. All these contributions to the free energy, while quantitatively important, are secondary to those responsible for the transformation (first-order phase transition) from one aggregation geometry to another, as compared with the internal (packing and mixing) contributions to the free energy. More explicitly, the free energies and free energy changes corresponding to the terms accounting for translational entropy, polydispersity, or interaggregate interactions are on the order of *kT per aggregate*. On the other hand, as we shall see below, the internal free energies are of order *kT per molecule*.

2. Model

The coexisting vesicles and micelles are treated, respectively, as an infinite planar bilayer (for which the two principal radii of curvature are $R_1 = R_2 = \infty$ everywhere) and an infinitely long cylinder of radius R, comparable to a molecular length. For every lipid–surfactant composition, the thickness of the bilayer or the radius of the cylindrical micelle are determined by minimizing the aggregate free energy. Since the thickness (radius) of the aggregate and the average area per molecule are related by the uniform density constraint, this minimization also determines the average optimal area per head group, a. An *ideal* entropy of mixing is assumed for both geometries.

2.1. Free Energy. Consider a bilayer or a cylinder containing $N = N_S + N_L$ molecules, with N_S and N_L denoting the number of surfactant and lipid molecules, respectively. The hydrophobic core of the aggregate, to a good approximation, is liquid-like[20-22] (uniformly packed with hydrocarbon chain segments). It can thus be regarded as an incompressible fluid phase, of volume $V = N_L v_L + N_S v_S$, with v_L, v_S denoting, respectively, the volumes of the lipid and surfactant tails.

The Helmholtz free energy of the system, F, is expressed in the form

$$f = F/N = x f_L(x) + (1-x) f_S(x) + k_B T[x \ln x + (1-x)\ln(1-x)] \quad (1)$$

where $x = x_L = N_L/N$ and $1 - x = x_S$ are the mole fractions of lipid and surfactant molecules, respectively. The first two terms in (1) are the internal free energy contributions with $f_L(x)$ ($f_S(x)$) representing the free energy per lipid (surfactant) molecule in an aggregate of composition x.

The last term represents the (ideal) mixing entropy. It should be noted that this term accounts only for the (supposedly random) *lateral* distribution of the amphiphile head groups at the hydrocarbon–water interfacial region; the chain conformational entropy contributions (which, say, according to the Flory-Huggins theory,[23] also con-

(14) Jennis, R. B. *Biomembranes: Molecular Structure and Function*; Springer: New York, 1989.
(15) Edwards, K.; Almgren, M. *J. Colloid Interface Sci.* **1991**, *147*, 1.
(16) Andelman, D.; Kozlov, M. M.; Helfrich, W. *Europhys. Lett.* **1994**, *25*, 231.
(17) Helfrich, W.; *Z. Naturforsch. C* **1973**, *28*, 693. See also: Helfrich, W. In *Physics of Defects, Les Houches Session XXXV*; Balian, R., Kleman, M., Poirier, J. P., Eds.; North Holland: Amsterdam, 1981. Evans, E. A.; Skalak, R. *CRC, Crit. Rev. Bioeng.* **1984**, *3*, 181. Petrov, A. G.; Bivas, J. *Prog. Surf. Sci.* **1984**, *16*, 389.
(18) For reviews of this approach, see e.g., Ben-Shaul, A.; Gelbart, W. M. in ref. 1c, Ben-Shaul, A. in ref. 1e; For its application to calculate, e.g., curvature elastic constants of membranes, see Szleifer, I.; Kramer, D.; Ben-Shaul, A.; Gelbart, W. M.; Safran, S. A. *J. Chem. Phys.* **1990**, *92*, 6800, solute-lipid interactions: Fattal, D. R., Ben-Shaul, A. *Biophys. J.* **1993**, *65*, 1795.
(19) Szleifer, I.; Ben-Shaul, A.; Gelbart, W. M. *J. Chem. Phys.* **1987**, *86*, 709.
(20) Israelachvili, J. N.; Mitchell, D. J.; Ninham, B. W. *J. Chem. Soc. Faraday Trans. 2* **1976**, *72*, 1525; Israelachvili, J. N. *Intermolecular and Surface Forces*; Academic Press: London, 1985.
(21) Tanford, C. *The Hydrophobic Effect*, 2nd ed.; Wiley-Interscience: New York, 1980.
(22) Wennerström, H.; Lindman, B. *Phys. Rep.* **1980**, *52*, 1.
(23) See: Hill, T. L. *Introduction to Statistical Thermodynamics*; Addison-Wesley: Reading, MA, 1960.

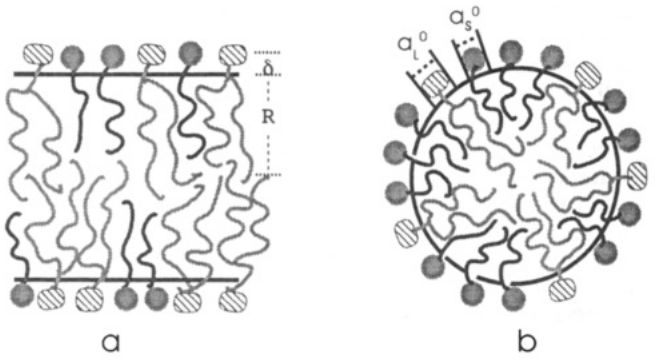

Figure 1. Schematic illustration of lipid and surfactant packing in a planar bilayer (a) and in a cylindrical micelle (b). The bare head group areas of lipid and surfactant are a_L^0 and a_S^0, respectively; R denotes the bilayer half-thickness or the cylinder radius (which are generally different), δ is the distance of the plane of head group repulsion from the surface of the hydrophobic core. The cylinder radius is larger than the surfactant tail length and comparable to the length of the longer lipid chain. The average area per surfactant head group can be significantly smaller than in a pure surfactant cylindrical micelle.[19]

tribute to the mixing entropy) are included in f_L and f_S, as detailed below. Note also that if the head groups were forming an incompressible 2D array at the interface, a more appropriate representation of the last term in (1) should involve the area fractions[16,19] ϕ rather than the mole fractions x; the lipid area fraction is given by $\phi = xa_L^0/[xa_L^0 + (1 - x)a_S^0]$ with a_L^0 and a_S^0 denoting the "bare" head group areas of lipid and surfactant, respectively. However, in general the total interfacial area exceeds the area covered by the head groups, i.e., $N_S a_S^0 + N_L a_L^0 < A$, where A is the total interfacial area. Also, since a_L^0 and a_S^0 are often comparable (e.g. for the OG/PC system), we shall express the translational (mixing) free energy in terms of the mole fractions, as in (1).

We calculate the lipid internal free energy as a sum

$$f_L(x) = f_L^s(x) + f_L^h(x) + f_L^t(x) \tag{2}$$

with the three terms accounting, respectively, for the hydrocarbon–water interfacial energy, head group–head group repulsions, and the conformational free energy of the hydrophobic tails (which includes interchain repulsions). The surfactant free energy $f_S(x)$ is defined analogously.

2.2. Surface and Head Group Contributions. For f_L^s we use[20,21]

$$f_L^s(x) = \gamma(a - a_L^0) \tag{3}$$

Here γ denotes the hydrocarbon–water surface tension and $a = a(x) = A/(N_S + N_L)$ is the average area per head group, measured at the hydrocarbon–water interface. The constant a_L^0 denotes the interfacial hydrocarbon–water area which is screened by the lipid head group and thus excluded from water–hydrocarbon contact; see Figure 1. We assume that a_S^0 is equal to the bare, hard core area of the amphiphile head group. An expression similar to (3) is used for $f_S^s(x)$.

The effective surface tension γ between the hydrophobic core and the surrounding solution is taken in all calculations as $\gamma = 0.12k_BT/\text{Å}^2$ at room temperature ($0.12k_BT/\text{Å}^2 \simeq 50$ erg/cm^2). The numerical values of a_L^0 and a_S^0 used in the calculations are detailed in section 3.

The repulsive interaction between the amphiphile polar heads involves steric ("hard-core") forces and, for ionic or zwitterionic head groups, also electrostatic forces. The absolute and relative magnitudes of these interactions vary from one system to another and are considerably more complex in mixed aggregates. Since the vesicle–micelle transition has been observed in a variety of systems, and in order to limit the number of adjustable parameters to a minimum, we have chosen to represent the repulsive interaction by a single functional form, applicable to both the planar and cylindrical aggregation geometries and for all lipid/surfactant rations. Thus, we write

$$f_L^h(x) = f_S^h = -k_BT \ln(1 - a^0/\bar{a}) \tag{4}$$

where $a^0 = xa_L^0 + (1 - x)a_S^0$ is the average "hard core" head group area per molecule, at the plane of head group interactions. We assume that this plane is sharply located at distance δ from the hydrocarbon–water interface. The average area per molecule, measured at this plane, is $\bar{a}$ (Figure 1). For a planar bilayer $\bar{a} = a$, whereas for a cylinder of (hydrophobic) radius R, $\bar{a} = (1 + \delta/R)a$.

Clearly, the van der Waals-like repulsion (4) is strictly appropriate only for steric repulsion[24,25] (as is the case, for instance, for octyl glucoside). Other forms, e.g. a capacitor-like model,[20–22,24] would be more appropriate to represent the dipolar interaction between zwitterionic lipids, yet this would imply additional adjustable parameters which at the level of the present analysis we would like to avoid. Thus, instead, (4) should be regarded as an empirical form in which the two important molecular parameters a_L^0 and a_S^0 are chosen such as to ensure that a pure lipid system prefers the planar bilayer geometry, whereas the surfactant spontaneous aggregation geometry is that of a cylindrical (or spherical) micelle (see section 3). It may be noted however that when (4) is expanded as a virial series (in powers of $1/a$) it implies $B_2 \sim a^0$ and $B_3 = (B_2)^2 \sim (a^0)^2$. Interestingly, a rather detailed model of lipid head group interactions (ref 26) suggests that indeed $B_3/(B_2)^2 \sim 1$ for both zwitterionic and nonionic lipids, a conclusion supported by experiments on pressure–area isotherms of such lipid monolayers. Thus, while seemingly appropriate only for steric repulsions, (4) may be regarded as a reasonable representation of head group repulsions for a wider class of lipids.

In the calculations described in the next section we have fixed the value of a_L^0 and treated a_S^0 and δ as molecular packing parameters which tune the spontaneous curvature of the aggregate. Qualitatively, for a surfactant of a given tail length, larger a_S^0 implies stronger head group repulsions, hence favoring the cylindrical over the planar bilayer geometry. Similarly, a shorter surfactant tail also favors the higher curvature due to smaller interchain repulsions. Larger δ results in larger $\bar{a}$ and hence reduced head group interaction energy. On the other hand, when δ increases, the distance between the plane of head group repulsions and the hydrocarbon–water interface also increases, thus favoring higher curvature. These two effects partly compensate each other and we expect a smaller effect of varying δ on the phase transition characteristics.

2.3. Chain Free Energies. The contribution of the hydrocarbon tails to the free energy is calculated using a molecular mean-field theory whose details and applications have been described elsewhere (see refs 18, 19, and 27). In this section we shall briefly outline its application to the calculation of conformational chain properties in mixed aggregates. The basic, and only, assumption in

(24) Nagarajan, R. *Langmuir* **1985**, *1*, 331.
(25) Puvvada, S.; Blankschtein, D. *J. Phys. Chem.* **1992**, *96*, 5579.
(26) Stigter, D.; Mingins, J.; Dill, K. A. *Biophys. J.* **1992**, *61*, 1616.
(27) Fattal, D. R.; Ben-Shaul, A. *Biophys. J.* **1994**, *67*, 983.

this theory is that the chain segment (monomer) density within the hydrophobic core is uniform, consistent with the observation that the core is liquid-like. This assumption can be cast as a constraint on the probability distributions of chain conformations within the hydrophobic region.

Consider first the case of a planar bilayer of composition x, which we shall assume to be the same in both monolayers. Let $P_L(\alpha)$ denote the probability of a lipid tail, originating from one of the two bilayer interfaces, to be in one of its possible conformations α. By symmetry, $P_L(\alpha) = P_L(\bar{\alpha})$ with $\bar{\alpha}$ denoting the mirror image of this conformation, with respect to the midplane, $z = 0$, and corresponding to a chain originating from the opposite interface. Also, let $\phi_L(\alpha,z)\,dz$ denote the volume taken up by an L-tail in the α conformation within the narrow shell $(z, z + dz)$, parallel to the bilayer midplane ($z = 0$). $(\phi_L(\alpha,z) = v\psi_L(\alpha,z)$ where $\psi_L(\alpha,z)$ is the number of segments of an (L,α)-tail within $(z, z + dz)$ and v is the average volume per chain segment. For a CH_2 group $v \simeq 27$ Å^3). Then, if the chain segment density is uniform throughout the hydrophobic interior of the bilayer,

$$x\sum_{\alpha}P_L(\alpha)[\phi_L(\alpha,z) + \phi_L(\alpha,-z)] + (1-x)\sum_{\beta}P_S(\beta)[\phi_S(\beta,z) + \phi_S(\beta,-z)] = a \quad (5)$$

Here $a = A/N$, the average cross sectional area per head group (either S or L) at either one of the two bilayer interfaces. Since the hydrophobic core is treated as an incompressible fluid, $a = (xv_L + (1-x)v_S)/d$ where d is the bilayer half-thickness. Note that the two terms in the square brackets in (5) represent the contributions to the segment density at z due to chains anchored at opposite interfaces. Chain interdigitation is mainly important around the midplane, $z = 0$, where $\phi_L(\alpha,z)$ and $\phi_L(\alpha,-z)$ are comparable. Near the interfaces, i.e., at $z \simeq \pm d$, only one of the terms is important.

A chain conformation (α) is fully specified by the positions of all atoms along the chain. In the rotational isomeric state (RIS) model[28] an equivalent specification is obtained in terms of the isomeric states of the bonds along the chain [the *trans–gauche* sequence in the case of simple alkyl chains $(CH_2)_{n-1}CH_3$]. In this latter scheme, used in the calculations reported in the next section, one also needs to specify the position of the zeroth segment (the chain origin or the "head group") relative to the hydrocarbon–water interface of the aggregate. To account for some roughness of the interface, we allow the chain origin to fluctuate within a narrow region (~2 Å) around the surface dividing between the hydrophobic and aqueous regions. Note that $P(\alpha)$ and $P(\beta)$ are invariant with respect to translations parallel to the bilayer plane or along or around the cylinder envelope.

The analogue of (5) for a mixed cylindrical micelle of radius R is

$$x\sum_{\alpha}P_L(\alpha)\,\phi_L(\alpha,r) + (1-x)\sum_{\beta}P_S(\beta)\,\phi_S(\beta,r) = ar/R \quad (6)$$

where r is the radial distance from the cylinder central axis, and a is again the average area per head group at the surface of the hydrophobic core. $\phi_L(\alpha,r)dr$ is the volume occupied by the segments of an (L,α)-chain in the cylindrical shell $(r, r + dr)$.

The average free energy per chain, in the mean-field approximation, is given by

$$f^t = x[\sum_{\alpha}P_L(\alpha)\,\epsilon_L(\alpha) + k_BT\sum_{\alpha}P_L(\alpha)\ln P_L(\alpha)] + (1-x)[\sum_{\beta}P_S(\beta)\,\epsilon_S(\beta) + k_BT\sum_{\beta}P_S(\beta)\ln P_S(\beta)] \quad (7)$$

where $\epsilon_L(\alpha)$ denotes the internal (*gauche*) energy of an L-chain in conformation α, and $\epsilon_S(\beta)$ is the internal energy of an (S,β)-chain.

The probability distributions $P_L(\alpha)$ and $P_S(\beta)$ for the bilayer and the cylinder are obtained by minimizing (7), with respect to (5) and (6), respectively. The functional form of the distributions, in both cases, is the same:

$$P_L(\alpha) = \frac{1}{q_L}\exp\{-[\epsilon_L(\alpha) + \int\pi(z)\,\phi(z;\alpha)\,dz]/k_BT\} \quad (8)$$

with a similar expression for $P_S(\beta)$. The $\pi(z)$ for the bilayer and the $\pi(r)$ for the cylinder are the Lagrange multipliers conjugate to the packing constraints. They depend on the composition and the aggregation geometry, since they are determined by the packing constraints; (5) for the bilayer, (6) for the cylinder. Note that $\pi(z)$ is the same for both types of chains in the same aggregate. The partition function q_L (and similarly q_S) is given by

$$q_L = \sum_{\alpha}\exp\{-[\epsilon_L(\alpha) + \int\pi(z)\,\phi(z;\alpha)dz]/k_BT\} \quad (9)$$

Substituting (8) into (7), we find

$$f^t = xf_L^t + (1-x)f_S^t = -k_BT[x\ln q_L + (1-x)\ln q_S] - \int\pi(z)\langle\phi(z)\rangle\,dz \quad (10)$$

with $\langle\phi(z)\rangle = x\langle\phi_L(z)\rangle + (1-x)\langle\phi_S(z)\rangle$; $\langle\phi_L(z)\rangle = \sum_\alpha P_L(\alpha)\,\phi_L(\alpha,z)$. Note that for the bilayer $\langle\phi(z)\rangle = a$ and for the cylinder $\langle\phi(r)\rangle = (r/R)a$.

The lateral pressure profile, $\pi(z)$, is calculated by a numerical solution of the packing constraints. The numerical procedure has been discussed in some detail elsewhere.[18,19] We only mention that it involves generation of all available conformations of the L and S chains and their classification into groups of degenerate conformations, i.e. of the same $\phi(\alpha;z)$. This yields a set of coupled nonlinear equations which can be solved numerically by standard procedures.

2.4. Geometric Packing Considerations. Simple geometric packing considerations impose limits on the possible values of the head group area, a, in single component micellar aggregates.[20,21] For instance, it is easy to show that $a \geq kv/l$ with $k = 3$, 2, and 1 for spherical micelles, cylindrical ones, and planar bilayers, respectively; where v and l denote the volume and contour length of the hydrocarbon chain. With $v \cong 27\,(n+1)$ Å^3 and $l \simeq 1.27\,n$ Å for simple alkyl tails, of the form $(CH_2)_{n-1}CH_3$, one finds (e.g. for $n = 15$) $a \geq 68$, 45, and 22.5 Å^2 for spheres, cylinders, and bilayers, respectively.

Similar, though slightly more involved, geometrical considerations[19] can be used to derive appropriate limits on $a = a(x)$ for binary aggregates of composition x. These considerations show that in, say, binary cylindrical aggregates composed of amphiphiles with different chain lengths the average area per head group may be considerably smaller than the minimal value $a \simeq 45$ Å^2 appropriate for pure cylindrical micelles. These basic, but important, notions must be taken into account in calculating $f = f(x)$.

More generally it should be noted that for aggregates of given composition and curvature (cylinders vs bilayers in our case) there is a wide range of possible head group

(28) Flory, P. J. *Statistical Mechanics of Chain Molecules*; Wiley-Interscience: New York, 1969.

areas, a. In all the calculations presented in section 3, the cylinder free energy, $f^c(x)$, and the bilayer free energy, $f^b(x)$, correspond to the minimum of the total free energy (1) with respect to a. The optimal (*equilibrium*) head group area is a function of both composition and curvature.

2.5. Phase Coexistence. Let $F^b = N^b f^b$ denote the bilayer free energy with f^b given by (1) and $N^b = N_L^b + N_S^b$. Similarly, $F^c = N^c f^c$ denotes the free energy of $N^c = N_L^c + N_S^c$ molecules packed in a cylindrical micelle. Treating the two systems as incompressible fluid phases, the conditions for phase equilibrium at a given temperature (T) are $\mu_L^c(x^c) = \mu_L^b(x^b)$ and $\mu_S^c(x^c) = \mu_S^b(x^b)$ with $\mu_L^c = (\partial F^c/\partial N_L^c)_{N_S^c}$, etc., denoting the chemical potentials of the two components. These conditions yield the common tangent equations

$$\left.\frac{\partial f^b}{\partial x}\right|_{x=x^b} = \left.\frac{\partial f^c}{\partial x}\right|_{x=x^c} \tag{11}$$

$$f^b(x^b) - x^b\left.\frac{\partial f^b}{\partial x}\right|_{x=x^b} = f^c(x^c) - x^c\left.\frac{\partial f^c}{\partial x}\right|_{x=x^c} \tag{12}$$

In the calculations presented in the next section these equations have been solved numerically to obtain x^b and x^c, the bilayer and cylinder compositions at coexistence.

3. Results

Considering the approximations involved in our model and the uncertainty with respect to some of the relevant molecular parameters (as well as the variance in the experimental data), the numerical examples presented in this section are not intended to reproduce a particular experimental result. Rather, our aim is to demonstrate how the basic trends characterizing the vesicle–micelle transition are driven by changes in molecular composition. Nevertheless, to illustrate our calculations we shall often refer to the egg phosphatidylcholine (PC)/octyl glucoside (OG) system which has been studied extensively by several experimental groups.[3,9-12]

Free energies were calculated for mixed vesicles (planar bilayers) and cylindrical micelles composed of doubly chained lipids of the form P_L–$[(CH_2)_{15}CH_3]_2$ and single (short) tail surfactants, P_S–$(CH_2)_7CH_3$. The lipid head group P_L includes the phosphatidylcholine moiety and the glycerol backbone. The latter can be regarded as marking the interface between the aqueous and hydrophobic regions. The surfactant polar head group is denoted by P_S. We have also performed, for comparison, some calculations for mixtures containing the same lipid but with a longer chain surfactant: P_S–$(CH_2)_{11}CH_3$, with the same head group as the C_8 surfactant.

3.1. Tail Free Energy. Chain conformations of lipid and surfactant tails were generated and classified according to the rotational isomeric state model.[28] The *gauche* energy was taken as 500 cal/mol and the temperature is T = 300 K. In modeling the chain statistics of the lipid molecules, the interactions between the two hydrocarbon tails emanating from the same head group were treated as equivalent to those between chains belonging to different head groups. This procedure provides a good approximation to the chain packing characteristics in bilayers composed of double-tailed lipids.[27]

Figure 2a shows the chain contributions, $f^t = xf_L^t(x) + (1 - x)f_S^t(x)$, for bilayers and cylinders as a function of a for several values of x; $a = A/(N_L + N_S)$ being the average area per head group at the hydrocarbon–water interface and $x = N_L/(N_L + N_S)$ is the mole fraction of the lipid in the aggregate. The mixed aggregates denoted by $(C_{16})_2$/C_8 are composed of lipids with two C_{16} chains and surfactants with a single, C_8, chain. Similarly, in Figure 2b, corresponding calculations for a $(C_{16})_2/C_{12}$ mixture are shown. All conformational chain free-energies are measured relative to those of the fully extended chains, for which the conformational entropy is zero (only the *all-trans* conformation is possible) and the total (*gauche*) energy is zero.

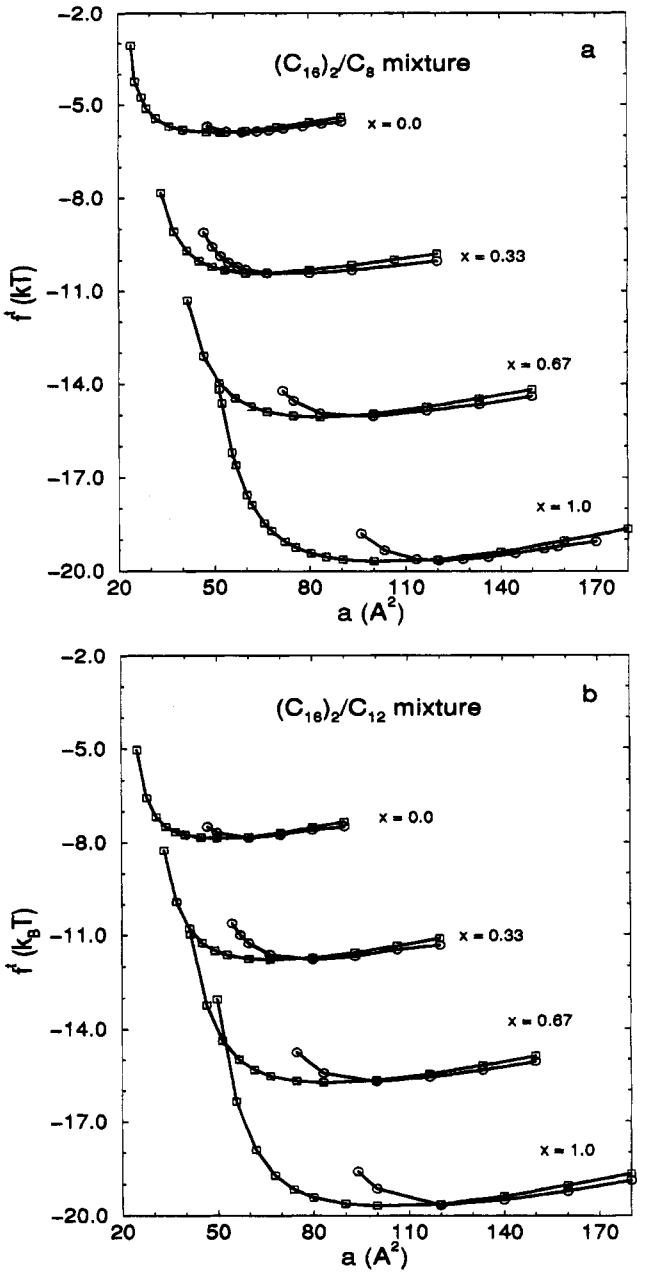

Figure 2. The tail contribution to the free energy per molecule, f^t (see eq 10), in a planar bilayer (squares) and a cylindrical micelle (circles) as a function of the average area per chain. The mole fraction of lipid molecules in the mixed aggregates is denoted by x. The bilayer and cylinder are composed of double-chained C_{16} lipids and single-chain surfactants. The surfactant tail in part a is a $(CH_2)_7CH_3$ chain and in part b it is a $(CH_2)_{11}$-CH_3 chain.

In a pure lipid system ($x = 1$) or a pure surfactant system ($x = 0$), simple geometric packing constraints (surface/volume ratios) imply that the average area per alkyl chain, a_c, must satisfy $a_c \geq 2v/l \simeq 45$ Å^2 for the cylinder and $a_c \geq v/l \simeq 22$ Å^2 for the bilayer. Note that for the surfactant $a_c = a_S$ while for the lipid $a_c = a_L/2$. The cross sectional area of one fully extended alkyl chain is approximately 22 Å^2. In Figure 2 this behavior corresponds to a steep rise in the free energy as a_c approaches these values. In the

bilayer $a_c \geq 22$ Å^2 holds also for the mixed system, but in the cylindrical geometry a_c can become significantly lower than ~ 45 Å^2 (see ref 18). In all cases, however, the (shallow) minima of the chain free energy curves correspond to a_c values which, due to interchain repulsion, are significantly larger than the above lower bounds.

3.2. Adding Head Group and Surface Contributions. The chain contribution to the free energy of a planar bilayer of composition x^b was calculated for a wide range of possible head group areas using (10). After adding the surface and head group contributions to the internal free energy, the optimal head group area, $a^* = a^*(x)$, was determined by minimizing (1) with respect to a. This yields $f^b(x) = f^b(x,a^*(x))$ and $f^c(x) = f^c(x,a^*(x))$ for the internal free energy in the bilayer and cylinder, respectively.

In all calculations we have used $\gamma = 0.12 k_B T$/Å$^2 \simeq 50$ erg/cm^2; cf. (3). The other relevant parameters, namely a_L^0, a_S^0, and δ were chosen as follows. In all the calculations presented below we have used $a_L^0 = 42$ Å^2. For the pure lipid bilayers, this yields $a_L^* \simeq 68$ Å^2 as the equilibrium area per molecule, similar to the experimental value reported in ref 10.

The choice of the parameters a_S^0 and δ appropriate for comparison with the experiment[9-12] is not obvious. In ref 10 it is suggested that the average head group area of OG is 38 Å^2. However, independent measurements on pure OG–water systems indicate that above the cmc OG forms small spheroidal micelles.[13,14] Hence, from simple packing considerations the average area per head group in these micelles should be at least 70 Å^2 ($\sim 3v/l$). If at higher concentrations the spherical micelles grow into cylinders the optimal head group area might be smaller than $\sim$70 Å^2 but not less than $\sim$46 Å^2 ($\sim 2v/l$). Accordingly, we have repeated the calculations for four different values of a_S^0: 40, 50, 60, and 70 Å^2.

The parameter δ, measuring the distance between the (average) plane of head group repulsion and the hydrocarbon–water interface, can be estimated from size measurements of the spheroidal OG micelles. It was found that the micelles formed at the cmc contain, on the average, 27 molecules, and their average radius can be estimate as 13.75 Å. The radius of the hydrophobic core can be calculated and was found to be 11.61 Å, suggesting that the average thickness of the polar region is 2.14 Å. Assuming that the plane of head group repulsion is in the center of this region we find $\delta = 1.07$ Å. In addition to this value, we performed calculations for $\delta = 1.5$ and 2.0 Å. As noted in the previous section, larger a_S^0 values favor higher (*spontaneous*) curvature. Thus, we expect the bilayer–micelle transition to occur at lower $(1 - x^b)$ as a_S^0 increases. Similarly, we expect $(1 - x^b)$ to be lower for surfactants with shorter tails. Increasing δ also leads to lower $(1 - x^b)$. However, as noted in section 2.2, the effect of varying δ is expected to be smaller than that of varying a_S^0.

Some typical calculations illustrating the dependence of the internal free energy on the average area per molecule in the two aggregation geometries are shown in Figure 3. Figure 3a shows the internal free energy per molecule in a pure $(C_{16})_2$ lipid aggregate, using $a_L^0 = 42$ Å^2. As mentioned above and clearly seen in the figure, this value yields $a_L^* \simeq 68$ Å^2 as the optimal area per head group in the bilayer.

For comparison, we also show in Figure 3a the free energy per lipid molecule in a cylindrical micelle, for the same a_L^0 and three different values of δ, namely, $\delta = 1.07$, 1.5, and 2 Å. The weak dependence on δ reflects the secondary role of head group repulsion (compared to the chain repulsion and surface tension terms) in determining the optimal area per lipid head group in the cylinder. The dashed vertical line at $a \simeq 90$ Å^2 marks the lowest possible interfacial area per lipid molecule in a cylinder.

Figure 3b shows how the free energy per molecule varies with a in pure surfactant aggregates. These calculations correspond to the case $a_S^0 = 50$ Å^2 and, again, for the three choices of δ used in Figure 3a. Clearly, in the bilayer the allowed values of a are $a \leq a_S^0$. In the cylinder $a(1 + \delta/k) \geq a_S^0$ so that a can be somewhat larger than a_S^0. We note that in a pure surfactant micelle varying δ shows a more pronounced effect on the free energy, reflecting the larger head/tail size ratio in this case, as compared to a pure lipid aggregate.

In a mixed aggregate we expect an intermediate behavior, as confirmed by the results shown in Figure 3c for mixed systems of composition $x = 1/3$. The optimal areas per molecule are quite similar in both geometries.

3.3. Vesicle–Micelle Transition. After evaluating, for each geometry and composition, the internal free energy terms $xf_L(x) + (1 + x)f_S(x)$ corresponding to $a = a^*(x)$, we add the mixing entropy contribution and obtain $f = f(x)$. This calculation is performed separately for the vesicle (planar bilayer) and the micelle (cylinder). Figure 4 illustrates the results obtained for $(C_{16})_2/C_8$ aggregates for two typical cases: (a) $a_S^0 = 50$ Å^2, $\delta = 1.07$ Å and (b) $a_S^0 = 70$ Å^2, $\delta = 1.5$ Å. Similar calculations have been performed for other choices of a_S^0 and δ and for $(C_{16})_2/C_{12}$ mixtures. Figure 4 clearly demonstrates that the cylinder and bilayer free energies cross at some intermediate composition and that the curves are both convex, enabling a common tangent construction. For the choice of parameters used in Figure 4a, the lipid mole fractions at the phase transition are $x = 0.47$ and 0.29 in the bilayer and cylinder, respectively. These correspond to a surfactant/lipid mole fraction ratio $R = (1 - x)/x$ the values of which are $R_b = 1.1$ in the bilayer and $R_c = 2.5$ in the cylinder; in reasonable agreement with experimental results for the OG/PC system.[9-12] The composition ratios corresponding to the results shown in Figure 4b are $R_b = 0.3$ and $R_c = 1.4$. Here, due to the higher spontaneous curvature of the pure surfactant system (larger a_S^0 value), the bilayer is destabilized at a lower surfactant/lipid ratio.

Head group repulsion increases with a_S^0, and hence also the preference of the surfactant molecule for the curved, cylindrical geometry. For instance, increasing a_S^0 from 40 to 60 Å^2 (for $\delta = 1.07$ Å) results in an increase of the optimal area per head group in a pure surfactant aggregate ($x = 0$) from $a^* = 48$ to 64 Å^2 in the cylinder, and from $a^* = 48$ to 70 Å^2 in the bilayer. Similar trends are found for the mixed aggregates. For example, taking $x = 0.5$, a^* increases from 63 to 66 Å^2 and from 52 to 61 Å^2 in the cylinder and bilayer, respectively. Thus, generally we expect that the bilayer saturation composition R_b will decrease as a_S^0 increases. This trend is confirmed in Figure 5 which shows the variation of R_b and R_c with a_S^0, for a C_8/C_{16} mixture. The figure also illustrates the effect of increasing δ, the distance between the plane of head group repulsion and the hydrocarbon–water interface. As noted earlier, increasing δ implies an increase in the spontaneous curvature of the aggregate, since the plane of head group repulsion is farther away from the neutral surface. In the cylindrical geometry, this effect is partially compensated for by the fact that the average area per head group at the plane of repulsion also increases, thus lowering f^*; cf. (4). We note from Figure 5a that the experimental results for the OG/PC system ($R_b \sim 1, R_c \sim 3$) correspond in our model to $a_S^0 \sim 45$ Å^2 (for $\delta = 1.07$ Å).

Another molecular parameter which tunes the spontaneous curvature in a mixed aggregate is the difference

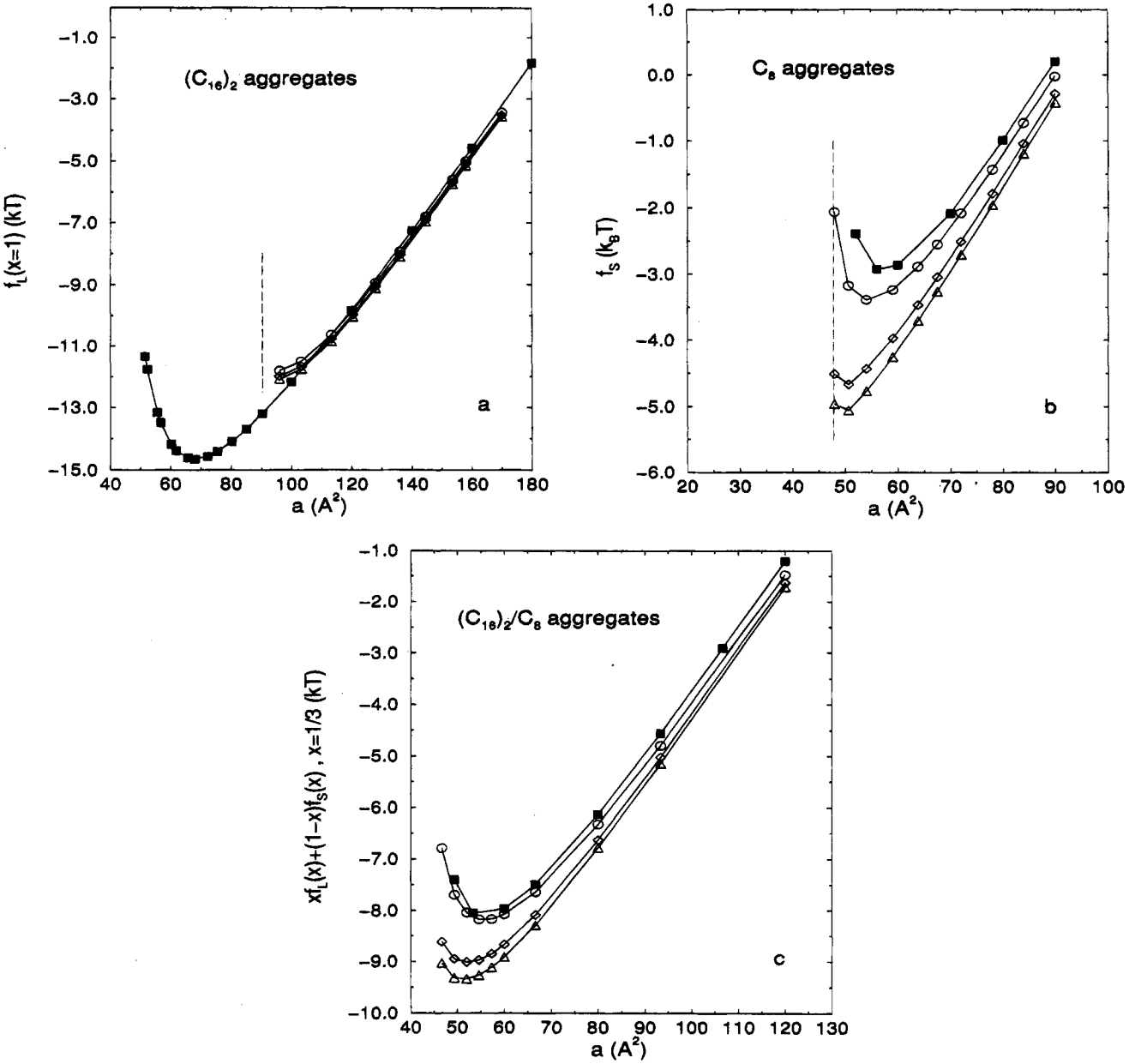

Figure 3. Average free energy per molecule including chain, surface tension, and head group contributions, as a function of the average area per molecule, measured at the hydrocarbon–water interface. (a) Pure lipid aggregates. Squares correspond to the planar bilayer geometry, and the other curves are for the cylindrical micelle; circles, diamonds, and triangles correspond to δ = 1.07, 1.5, and 2.0 Å, respectively. In all cases $a_L^0 = 42$ Å^2. The dashed line, at $a \simeq 90$ Å^2 marks the minimal area per lipid head group (two chains) in the pure cylindrical aggregate. (b) The average free energy per molecule in pure surfactant aggregates, for $a_S^0 = 50$ Å^2. Molecular parameters and symbols are as in part a. The dahsed line, at $a \simeq 48$ Å^2 marks the minimal area per surfactant head group in the pure cylindrical aggregate. (c) The average free energy per molecule in mixed (x = 1/3) bilayers and cylinders, as a function of the average area per molecule. Parameters and symbols as in parts a and b.

in chain length of the two amphiphilic chains. Larger disparity favors higher curvature.[19] We thus expect that C_{12} chains will be less effective in destabilizing a $(C_{16})_2$ bilayer than C_8 chains. Consequently, R_b is expected to be lower in the $(C_{16})_2/C_8$ system than in the $(C_{16})_2/C_{12}$ system (for the same set of head group interaction parameters). This prediction is confirmed by comparing the results for the $(C_{16})_2/C_8$ system and the $(C_{16})_2/C_{12}$ system in Figure 5.

A qualitatively similar behavior has been observed for mixtures of C_n/C_m carboxilic acids.[29] In this system it was found that a stable lamellar (bilayer) phase prevails at all compositions of C_{14}/C_{18} mixtures. On the other hand, in C_{10}/C_{18} mixtures, where chain disparity is significantly larger, the lamellar state is stable at high and low x_n/x_m ratios, but another phase (apparently cubic), characterized by higher curvature, prevails at intermediate concentrations.

(29) Charvolin, J.; Mely, B. *Mol. Cryst. Liq. Cryst.* **1978**, *41*, 209.

4. Concluding Remarks

It is well-known that the optimal packing (micellar) geometry of pure (single component) amphiphilic aggregates depends on the molecular characteristics of their constituents. In particular, the optimal, *spontaneous*, curvature of the aggregate depends on the relative *size* of the head groups and hydrocarbon tails, reflecting the strength of head group and intertail repulsion. In mixed aggregates the relative importance of these interactions varies with their molecular composition. First-order phase transitions can occur from one packing geometry to another, having different compositions (*order parameters*). The vesicle–micelle transition in lipid–surfactant mix-

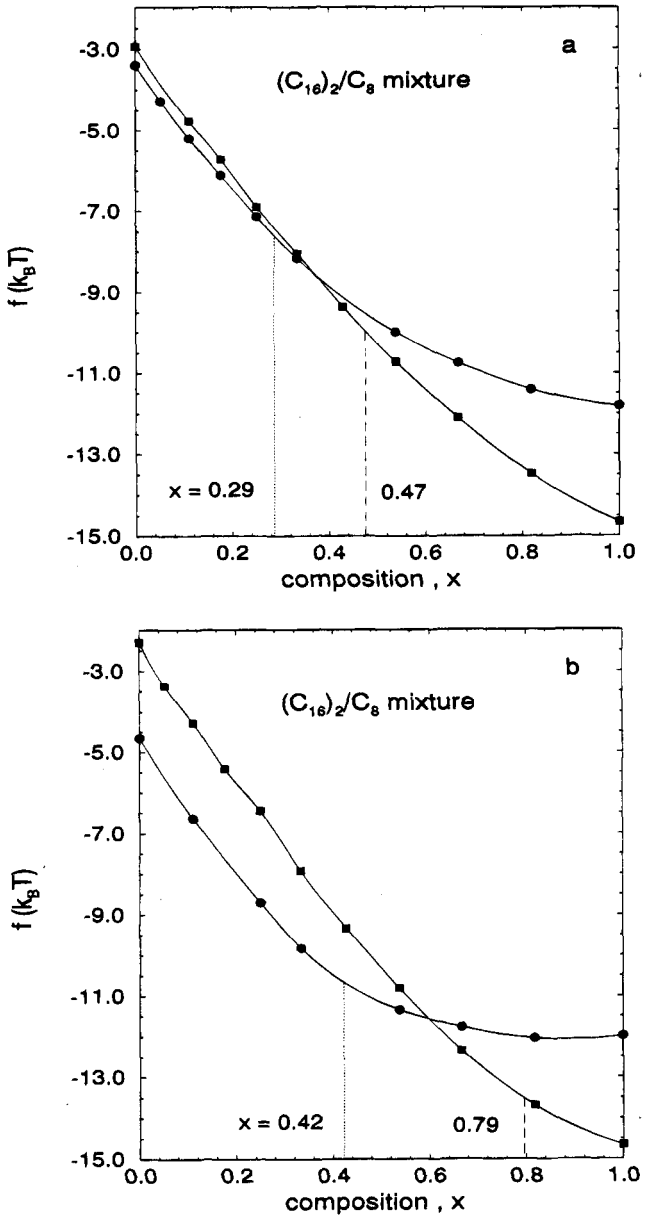

Figure 4. The average free energy per molecule (including all internal contributions and the entropy of mixing) in mixed aggregates composed of $(C_{16})_2$ lipids and C_8 surfactants as a function of lipid mole fraction. The squares correspond to the planar bilayer and the circles to the cylindrical micelle. The dashed and dotted vertical lines mark, respectively, the bilayer and cylinder compositions at the phase transition. The molecular parameters used are $a_S^0 = 50$ Å^2 and $\delta = 1.07$ Å in part a and $a_S^0 = 70$ Å^2 and $\delta = 1.5$ Å in part b. Note that as a_S^0 increases the bilayer → cylinder transition takes place at a lower surfactant mole fraction.

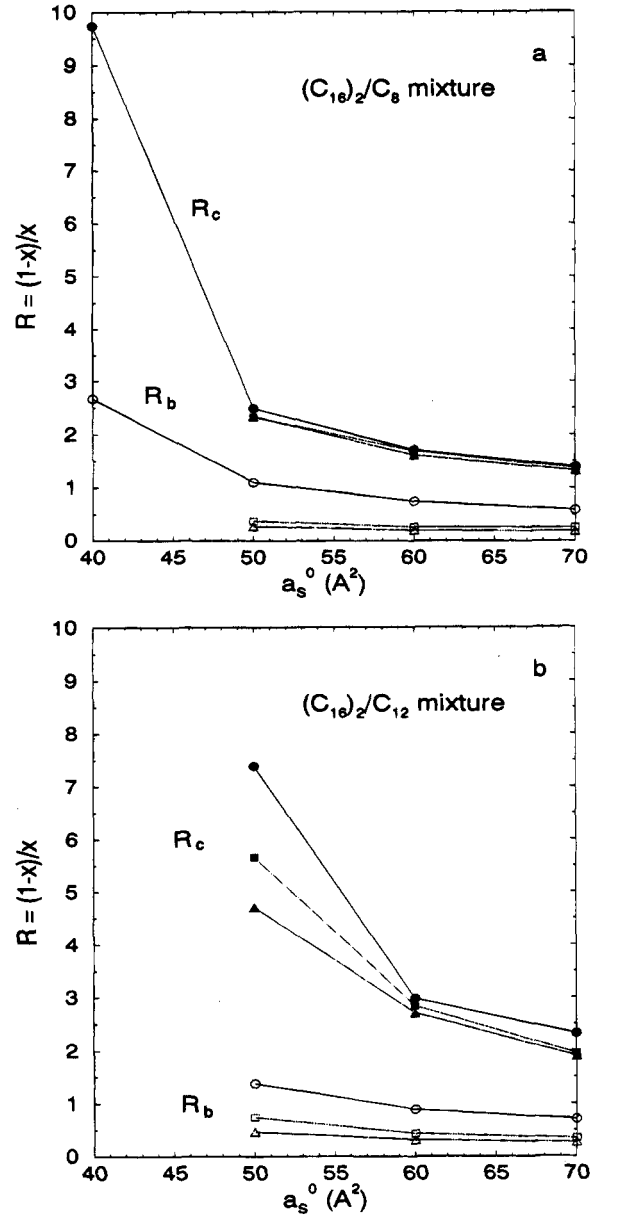

Figure 5. The surfactant/lipid mole fraction ratio, at coexistence, in the vesicle bilayer (open symbols) (R_b) and in the cylindrical micelle (solid symbols) (R_c) as a function of the surfactant "hard core" area, a_S^0. The circles, squares and triangles are for $\delta = 1.07$, 1.5, and 2.0 Å, respectively. The aggregates are composed of C_{16} lipids and C_8 surfactants in part a and C_{16} lipids and C_{12} surfactants in part B.

tures is one of the more well-studied examples of such composition-driven shape transitions. In this paper we have shown that a relatively simple molecular theory, incorporating both chain statistics (tail repulsions) and head group interaction, can account for the basic characteristics of the vesicle–micelle transition. The model can also predict some general trends associated with changes in certain relevant molecular parameters, such as head group size or chain length disparity. Of course, quantitative predictions would require more accurate modeling of the head group repulsions as well as consideration of the finite size of the aggregates (polydispersity, translational entropy, and edge effects) and interaggregate interactions.

Acknowledgment. We thank Bill Gelbart, Misha Kozlov, Dov Lichtenberg and Ishi Talmon for helpful discussions. The support of the National Science Foundation administered by the Israel Academy of Sciences and Humanities (A.B.-S. and D.A.), the Yeshaya Horowitz Association (A.B.-S.) and the German-Israeli Foundation (GIF) under Grant No. I-0197 (D.A.) is gratefully acknowledged. The Fritz Haber Center is supported by the Minerva Gesellschaft für die Forschung, mbH, Munich, Germany.

LA940796D